

Fault Location Approach to Distribution Networks Based on Custom State Estimator

Luis F. Ugarte, *Student Member, IEEE*, Madson C. de Almeida, *Member, IEEE*, and
Luís H. T. Bandória, *Student Member, IEEE*

Abstract—This paper presents a properly designed branch current based state estimator (BCBSE) used as the main core of an accurate fault location approach (FLA) devoted to distribution networks. Contrary to the approaches available in the literature, it uses only a limited set of conventional measurements obtained from smart meters to accurately locate faults at buses or branches without requiring measurements provided by phasor measurement units (PMUs). This is possible due to the methods used to model the angular reference and the faulted bus, in addition to the proper choice of the weights in the state estimator (SE). The proposed approach is based on a searching procedure composed of up to three stages: ① the identification of the faulted zones; ② the identification of the bus closest to the fault; and ③ the location of the fault itself, searching on branches connected to the bus closest to the fault. Furthermore, this paper presents a comprehensive assessment of the proposed approach, even considering the presence of distributed generation, and a sensitivity study on the proper weights required by the SE for fault location purposes, which can not be found in the literature. Results show that the proposed BCBSE-based FLA is robust, accurate, and aligned with the requirements of the traditional and active distribution networks.

Index Terms—Active distribution network, branch current based state estimator, fault location, smart meter.

I. INTRODUCTION

DISTRIBUTION networks typically have a radial topology consisting mainly of overhead lines, which makes them highly vulnerable to faults or short-circuits. Since a fault is the leading cause of power supply interruptions, the development of fault location approaches (FLAs) is of great interest to utilities to reduce interruption times, avoid deterioration of power quality indices, and improve the reliability of the network. Under fault conditions, the protection acts to

isolate the area affected by the fault. Therefore, it is necessary to identify and locate the fault to restore the power supply and maintain the power quality indices within the limits [1].

The advances in communication and metering infrastructures, required by active distribution networks (ADNs) [2], can significantly contribute to the wide adoption of automatic FLAs. The distribution management system (DMS) combines these technologies to operate distribution networks to improve power quality and reliability. To reduce the recovery time after a fault in a distribution network, the available approaches can be classified into FLAs and outage identification approaches (OIAs), as shown in Fig. 1.

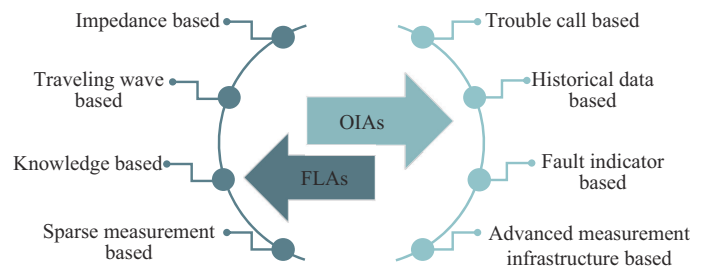


Fig. 1. Overview of FLAs and OIAs.

The impedance based approaches can be implemented in traditional distribution networks and ADNs. The main issues are the multiple fault location paradigm and the typical low accuracy, especially when facing unbalanced loads and distributed generation (DG) [3]-[7]. The traveling wave based approaches require a very high sampling rate for measurements, mainly when applied to distribution networks, since the accuracy of traveling wave based approaches may significantly deteriorate in three-phase systems with several laterals and short lines [8]-[12]. The knowledge based approaches exhibit low computational cost with short execution time and generalization capability. In contrast, this approach requires a large amount of data for the training process [13]-[17]. The sparse measurement based approaches consider recent advances in communication and metering devices and can cope with conventional non-synchronized as well as synchronized measurements [18]-[22].

These approaches are based on the fact that each fault causes voltage sags and current rises with different features. However, due to the errors inherent to the measurements, the delays in communication, the limited number of available

Manuscript received: July 29, 2022; revised: December 12, 2022; accepted: May 3, 2023. Date of CrossCheck: May 3, 2023. Date of online publication: June 14, 2023.

This work was supported in part by the grant #2021/11380-5, Centro Paulista de Estudos da Transição Energética (CPTEn), São Paulo Research Foundation (FAPESP); the grant #88887.661856/2022-00, Coordenação de Aperfeiçoamento de Pessoal de Nível Superior - Brasil (CAPES); and the grant #88887.370014/2019-00, Coordenação de Aperfeiçoamento de Pessoal de Nível Superior - Brasil (CAPES).

This article is distributed under the terms of the Creative Commons Attribution 4.0 International License (<http://creativecommons.org/licenses/by/4.0/>).

L. F. Ugarte (corresponding author), M. C. de Almeida, and L. H. T. Bandória are with the Department of Systems and Energy, State University of Campinas, Campinas, São Paulo 13083-970, Brazil (e-mail: l192702@dac.unicamp.br; madson@dsee.fee.unicamp.br; 1156449@dac.unicamp.br).

DOI: 10.35833/MPCE.2022.000470

measurements, the presence of distributed generators, the three-phase representation of the network, and the typical unbalanced loads, the state estimation approach can be used as a key tool to provide the estimates required for fault location purposes. Indeed, a sparse measurements based FLA supported by a properly designed state estimator (SE) that uses only conventional non-synchronized measurements is the main focus of this paper.

Given an adequate set of measurements and network data, SEs can provide the most likely state of a power system, even under fault conditions, enabling network managements [23], [24]. According to the literature, most of the SE-based FLAs consider phasor measurements for better performance [25]-[30]. In [25], an approach to locating the faulted branch is presented, which considers the weighted measurement residual as a metric. This approach uses a linearized SE, where the state variables are the complex bus voltages in rectangular coordinates. The measurement plan adopts only phasor measurements provided by phasor measurement units (PMUs) placed at all network buses. In [26] and [31], an approach devoted to locating the bus closest to the fault considering the Euclidean norm as a metric is presented. This approach uses an SE whose state variables are the complex bus voltages in rectangular coordinates and assumes that pseudo-measurements can be neglected during fault conditions. The measurement plan considers a limited number of phasor measurements. To assess the approach, tests were performed in real-time simulators [26]. In [27], an approach to locating the faulted branches and buses in an ADN with distributed generators considers measurement residuals as the metric. This approach uses a linearized SE, where the state variables are the complex bus voltages in rectangular coordinates. The ZIP and constant impedance models are adopted to represent power consumption and provide pseudo-measurements. Moreover, phasor measurements are considered at the substation and DG buses. In [29], FLA using SE where the state variables are the complex bus voltages in rectangular coordinates is presented along with an analysis of the required number of PMUs and their optimal placing, presenting difficulties in detecting and locating single-phase-to-ground faults. The metric of detection and localization is the weighted measurement residual.

Considering the branch currents as state variables, an approach to locating the nearest neighbor bus to the fault is proposed in [32]. This approach adopts the normalized residual as the metric, needing a very large measurement plan to guarantee the good performance of the approach. This measurement plan adopts both conventional as well as phasor measurements. In [30], an approach to locating the faulted branch is presented, which considers the normalized residual as the metric. First, this approach runs the SE to find the bus closest to the fault considering phasor measurements. Then, it calculates an angular index to identify the exact location of the fault on the branch. In [28], a graph-based faulted line location approach is proposed. This measurement plan adopts a limited number of phasor measurements. Based on the graph model of the reduced searching region, the SE is performed in a hierarchical structure to locate the

fault, considering the weighted measurement residual as the metric.

In summary, to the best of the author's knowledge, the literature presents approaches based only on synchronized measurements provided by PMUs, and the ones that use conventional non-synchronized as well as synchronized measurements provided by PMUs (used to improve accuracy). In this context, this paper proposes an approach that uses only a limited set of conventional non-synchronized measurements and a properly designed SE to improve the quality of the fault location without requiring measurements provided by PMUs.

The proposed approach adopts a branch current based SE (BCBSE) with proper methods to model the angular reference and the faulted bus, in addition to the adequate choice of the weights for the measurements and pseudo-measurements. Furthermore, under fault conditions, all the contributions of the shunt admittances of the branches are considered in modeling of equivalent current measurements. These modeling aspects are fundamental to achieving high accuracy in fault location without requiring measurements from PMUs. The proposed approach allows for accurately locating faults at buses or branches. The weighted sum of squared residuals $J(\mathbf{x})$ is used as the fault location index (FLI), which can be applied even in the presence of a reduced set of measurements, i.e., a redundant set of measurements is not required. The BCBSE is adopted because it results in a constant Jacobian matrix, which improves the overall computational performance. Furthermore, the proposed approach is based on a searching procedure composed of up to three stages: ① the identification of the faulted zone; ② the identification of the bus closest to the fault; and ③ the location of the fault itself, searching on branches adjacent to the bus closest to the fault. This procedure, together with the constant Jacobian matrix, results in a reduced computational burden, even considering that the computational time is not a hard constraint for FLAs. Moreover, this paper presents a comprehensive assessment of the proposed approach considers the presence of DGs, and also a sensitivity study on the weights required by the SE for fault location purposes, which to the best of the author's knowledge, can not be found in the literature.

The remainder of this paper is structured as follows. Section II describes the proposed BCBSE, highlighting a simple and accurate way to specify the angular reference and model the equivalent measurements. The proposed FLA, along with the modeling of the fault and the FLI, is detailed in Section III. In Section IV, the performance of the proposed FLA is assessed considering several case studies under fault conditions. Finally, the conclusions are drawn in Section V.

II. PROPOSED BCBSE

In a distribution network under normal conditions, the bus voltage magnitudes are close to the nominal values, and the voltage angles are typically small. Under these conditions, the classical state estimation methods are expected to perform very well [24]. On the other hand, under fault conditions, the voltages and currents can significantly deviate

from nominal values and may lead the methods to present convergence issues once these methods are solved via Gauss-Newton methods. In order to avoid that, FLAs based on SE typically assume the availability of PMUs and adopt a linear formulation. These linear SEs are solved by non-iterative (direct) procedures and, by definition, they can not present convergence issues even under severe fault conditions.

Given that PMUs are not expected to be widely available in distribution networks, the main idea in this paper is to use only conventional non-synchronized measurements obtained from smart meters and pseudo-measurements. For that, the so-called branch current based state estimator (BCBSE) is adopted, and a set of cautions in modeling is used to prevent convergence issues when running under fault conditions. Thus, special attention is given to the specification of the angular reference, the modeling of the voltage magnitude measurements, and the modeling of the fault condition.

A. Basic Algorithm of BCBSE

The state variables of the BCBSE are the real and imaginary parts of the voltages at the reference bus plus the real and imaginary parts of the branch currents, i.e., $(\mathbf{v}_{ref, re}, \mathbf{v}_{ref, im}, \mathbf{i}_{km, re}, \mathbf{i}_{km, im})$, where the subscript km denotes the branch connecting buses k and m ; the subscripts re and im denote the real and imaginary parts, respectively; and the subscript ref denotes the reference bus [33]. The measurement model for the BCBSE is shown in (1).

$$\mathbf{z}^{eq}(\mathbf{x}) = \mathbf{H}\mathbf{x} + \mathbf{e} \quad (1)$$

This linear relationship between the state vector \mathbf{x} and the equivalent measurement vector $\mathbf{z}^{eq}(\mathbf{x})$ leads to a constant Jacobian matrix \mathbf{H} , which is composed of system impedances, zeros, and ones, and vector \mathbf{e} contains the errors inherent to the measurements [33]. Indeed, the Jacobian matrix \mathbf{H} will be constant given that a proper representation of the voltage magnitude measurements is adopted [34], [35]. The weighted least square (WLS) solution for the state variables can be obtained via the Gauss-Newton method by iteratively solving the normal equation (2), where the equivalent measurements $\mathbf{z}^{eq}(\mathbf{x}^\eta)$ are updated at each iteration η . Furthermore, as the variances of the equivalent measurements can be assumed to be constant, as proposed in [34], the weighting matrix \mathbf{W} and, consequently, the gain matrix, $\mathbf{H}^T\mathbf{W}\mathbf{H}$, can also be kept constant during the iterative solution process. This simplifies the calculations and significantly reduces the computational burden of the state estimation process. The basic algorithm for the BCBSE is shown in Fig. 2, where \mathbf{x}^{est} is the estimated state. It can be observed that the gain matrix is built and factorized just once outside the iterative process.

$$\mathbf{x}^{\eta+1} = (\mathbf{H}^T\mathbf{W}\mathbf{H})^{-1} \mathbf{H}^T\mathbf{W}\mathbf{z}^{eq}(\mathbf{x}^\eta) \quad (2)$$

The conventional measurements in the state estimation process are the active and reactive power injections and power flows and the voltage magnitudes. For the BCBSE, these conventional measurements are converted into equivalent currents and voltages [33]. If PMUs are available, the measured complex voltages and currents are used directly without conversion.

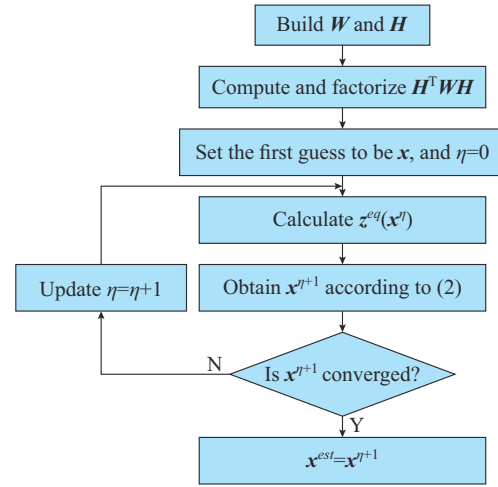


Fig. 2. Basic algorithm for BCBSE.

B. Equivalent Measurements

1) Equivalent Current Measurements

Consider a three-phase branch km with shunt admittances and loads connected at terminal buses k and m , as shown in Fig. 3. In obtaining the equivalent current injection measurements, the active and reactive power injections are measured at the loads. These power injections are then converted into equivalent current injections as shown in (3).

$$\begin{bmatrix} \vec{i}_k^{a,eq} \\ \vec{i}_k^{b,eq} \\ \vec{i}_k^{c,eq} \end{bmatrix} = \begin{bmatrix} i_k^{a,eq} + j i_{k,im}^{a,eq} \\ i_k^{b,eq} + j i_{k,im}^{b,eq} \\ i_k^{c,eq} + j i_{k,im}^{c,eq} \end{bmatrix} = \begin{bmatrix} \left(\frac{p_k^{a,mea} + j q_k^{a,mea}}{\vec{v}_k^{a,\eta}} \right)^* \\ \left(\frac{p_k^{b,mea} + j q_k^{b,mea}}{\vec{v}_k^{b,\eta}} \right)^* \\ \left(\frac{p_k^{c,mea} + j q_k^{c,mea}}{\vec{v}_k^{c,\eta}} \right)^* \end{bmatrix} - \mathbf{Y}_k \begin{bmatrix} \vec{v}_k^{a,\eta} \\ \vec{v}_k^{b,\eta} \\ \vec{v}_k^{c,\eta} \end{bmatrix} \quad (3)$$

where $\vec{i}_k^{j,eq}$ is the equivalent current injection of each phase j at terminal bus k ; $\vec{v}_k^{j,\eta}$ is the voltage phasor of each phase j at terminal bus k and iteration η ; $p_k^{j,mea}$ and $q_k^{j,mea}$ are the active and reactive power injections of each phase j at terminal bus k , respectively; and \mathbf{Y}_k is a 3×3 matrix containing the association of the shunt admittances of the branches \mathbf{Y}_{km}^{sh} and the shunt admittances connected to the buses \mathbf{Y}_k^{sh} . As a result, the vector $\mathbf{Y}_k \vec{v}_k^\eta$ contains the currents injected by the shunt elements at bus k .

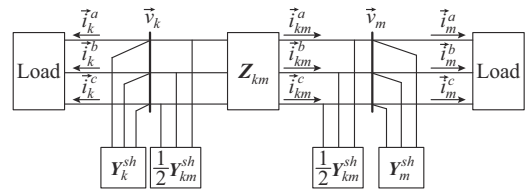


Fig. 3. General model of a three-phase distribution branch.

In a similar way, to obtain the equivalent current flow measurements, the active power and reactive power flowing through the branches are measured close to the terminal buses. These power flows are then converted into equivalent current flows as shown in (4).

$$\begin{bmatrix} \vec{i}_{km}^{a,eq} \\ \vec{i}_{km}^{b,eq} \\ \vec{i}_{km}^{c,eq} \end{bmatrix} = \begin{bmatrix} \vec{i}_{km, re}^{a,eq} + j\vec{i}_{km, im}^{a,eq} \\ \vec{i}_{km, re}^{b,eq} + j\vec{i}_{km, im}^{b,eq} \\ \vec{i}_{km, re}^{c,eq} + j\vec{i}_{km, im}^{c,eq} \end{bmatrix} = \begin{bmatrix} \left(\frac{p_{km}^{a,mea} + jq_{km}^{a,mea}}{\vec{v}_k^{a,\eta}} \right)^* \\ \left(\frac{p_{km}^{b,mea} + jq_{km}^{b,mea}}{\vec{v}_k^{b,\eta}} \right)^* \\ \left(\frac{p_{km}^{c,mea} + jq_{km}^{c,mea}}{\vec{v}_k^{c,\eta}} \right)^* \end{bmatrix} - \frac{1}{2} \mathbf{Y}_k^{sh} \begin{bmatrix} \vec{v}_k^{a,\eta} \\ \vec{v}_k^{b,\eta} \\ \vec{v}_k^{c,\eta} \end{bmatrix} \quad (4)$$

where $\vec{i}_{km}^{j,eq}$ is the equivalent current flow of each phase j on branch km ; and $p_{km}^{j,mea}$ and $q_{km}^{j,mea}$ are the active and reactive power flows of each phase j on branch km , respectively.

As observed in (3) and (4), both the active and reactive power measurements are required to obtain the equivalent current measurements. If either of the two power measurements is missing, a pseudo-measurement with adequate variance can be used. Note that (3) and (4) include all available phases. To represent single- and two-phase branches as three-phase elements, the concept of dummy nodes and dummy lines can be adopted [36]. Finally, if the shunt elements are discarded, (3) and (4) can be simplified, as presented in [33]-[35].

2) Equivalent Voltage Measurements

According to [35], at least four approaches can be found in the literature to represent voltage magnitude measurements in the BCBSE. Based on the results presented in [35], the approach proposed in [34] will be adopted in this paper because it results in constant coefficients in the Jacobian matrix. Moreover, as shown in this paper, it does not deteriorate the convergence of the BCBSE under fault conditions. As proposed in [34], the conversion of voltage magnitude measurements $v_k^{j,mea}$ into the equivalent voltage measurements $v_k^{a,eq}$, $v_k^{b,eq}$, $v_k^{c,eq}$ for each phase of bus k is done according to (5).

$$\begin{bmatrix} v_k^{a,eq} \\ v_k^{b,eq} \\ v_k^{c,eq} \end{bmatrix} = \begin{bmatrix} v_{k,re}^a \cos \phi_k^a \\ v_{k,re}^b \cos \phi_k^b \\ v_{k,re}^c \cos \phi_k^c \end{bmatrix} - \begin{bmatrix} v_{k,im}^a \sin \phi_k^a \\ v_{k,im}^b \sin \phi_k^b \\ v_{k,im}^c \sin \phi_k^c \end{bmatrix} \quad (5)$$

where $v_{k,re}^j = v_k^{j,mea} \cos \theta_k^\eta$ for each phase j ; $v_{k,im}^j = v_k^{j,mea} \sin \theta_k^\eta$ for each phase j ; and ϕ_k^j is the rotation angle, which is constant and equal to the angles of the bus voltages at the first guess of the BCBSE. The angle θ_k^η is used to artificially create a complex voltage measurement from the measured voltage magnitudes. It can be observed that this angle is updated at every iteration η of the solution process.

In BCBSE, as the state variables are the voltages of the reference bus and the branch currents, the equivalent voltage measurements need to be modeled as voltage drops from the reference bus ref to the measured bus k . For that, $v_{k,re}^j$ and $v_{k,im}^j$ in (5) are rewritten as (6) and (7), respectively.

$$\begin{bmatrix} v_{k,re}^a \\ v_{k,re}^b \\ v_{k,re}^c \end{bmatrix} = \begin{bmatrix} v_{ref}^a \cos \theta_{ref}^a \\ v_{ref}^b \cos \theta_{ref}^b \\ v_{ref}^c \cos \theta_{ref}^c \end{bmatrix} - \sum_{km \in \Omega_{krf}} \left(\mathbf{R}_{km} \begin{bmatrix} i_{km,re}^a \\ i_{km,re}^b \\ i_{km,re}^c \end{bmatrix} - \mathbf{X}_{km} \begin{bmatrix} i_{km,im}^a \\ i_{km,im}^b \\ i_{km,im}^c \end{bmatrix} \right) \quad (6)$$

$$\begin{bmatrix} v_{k,im}^a \\ v_{k,im}^b \\ v_{k,im}^c \end{bmatrix} = \begin{bmatrix} v_{ref}^a \sin \theta_{ref}^a \\ v_{ref}^b \sin \theta_{ref}^b \\ v_{ref}^c \sin \theta_{ref}^c \end{bmatrix} - \sum_{km \in \Omega_{krf}} \left(\mathbf{X}_{km} \begin{bmatrix} i_{km,re}^a \\ i_{km,re}^b \\ i_{km,re}^c \end{bmatrix} + \mathbf{R}_{km} \begin{bmatrix} i_{km,im}^a \\ i_{km,im}^b \\ i_{km,im}^c \end{bmatrix} \right) \quad (7)$$

where v_{ref}^j and θ_{ref}^j are the voltage magnitude and angle in a given phase j of the reference bus, respectively; Ω_{krf} is the set of branches connecting bus k to reference bus; $i_{km,re}^j$ and $i_{km,im}^j$ are the real and imaginary parts of the currents of each phase j on branch km , respectively; and $\mathbf{Z}_{km} = \mathbf{R}_{km} + j\mathbf{X}_{km}$ is the series impedance matrix of the branch km . Based on the above, the derivatives of the Jacobian matrix are obtained from (5), (6) and (7) and, therefore, the elements of the Jacobian matrix are constant. The values that go in $\mathbf{z}^{eq}(\mathbf{x}^\eta)$ are obtained from (5) and, hence, they are updated at every iteration η .

C. Weights for Equivalent Measurements

In power system state estimation under normal conditions, more accurate measurements are recommended to be associated with higher weights, and less accurate measurements such as pseudo-measurements are associated with lower weights. The inverse of the variances of the measurements is typically used as weight [23], [24].

In this paper, given that measurements are converted into equivalent measurements, considering the error propagation theory, the variances and covariances of the equivalent measurements are calculated from the variances of the measurements and used to compose the weighting matrix \mathbf{W} of the equivalent measurements [34], [37]. A detailed discussion on that, as well as the adopted equations, can be found in [34].

D. Angular Reference

According to [38], under normal conditions, the angular reference in distribution network SEs can be specified in two ways. In the first way, the angular reference is placed on the network substation. As only the voltage magnitudes are measured in the substation, voltage angles are assumed to be displaced at 120° . In the second way, the network upstream of the substation (*sub*) is represented by a Thevenin equivalent. Then, the angular reference is placed at an internal bus (*int*) of this equivalent. The idea is illustrated in Fig. 4. As this internal bus is, by definition, a balanced bus, it presents complex voltages with the same magnitude and displaced value of 120° , i.e., $v_{ref}^a = v_{ref}^b = v_{ref}^c$, $\theta_{ref}^b = \theta_{ref}^a - 120^\circ$, and $\theta_{ref}^c = \theta_{ref}^a + 120^\circ$. In this approach, the unbalances inherent to the distribution networks, or even the unbalances inherent to asymmetrical faults, are not masked and can adequately fit the measurements obtained under fault conditions. The impedance matrix \mathbf{Z}_s is obtained from the three- and single-phase short-circuit levels of the substation [38].

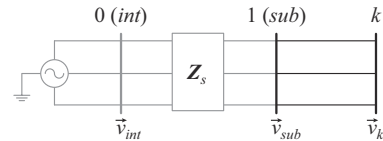


Fig. 4. Angular reference placed at internal bus of Thevenin equivalent representing network upstream of substation.

Given that under asymmetrical fault conditions the unbalances in currents and voltages can be severe, the second way is recommended in this paper. As it will be shown, it contributes to maintaining the good convergence features of the

BCBSE under asymmetrical fault conditions and allows a proper fitting to the available measurements.

E. Modeling Fault

In this paper, a fault at bus k is modeled by including pseudo-measurements representing the fault currents as injections at bus k . To consider the effect of the symmetrical or asymmetrical faults, these pseudo-measurements are included in all phases of bus k . The pseudo-measurements are obtained according to (8).

$$\begin{bmatrix} \vec{i}_k^{a,fault} \\ \vec{i}_k^{b,fault} \\ \vec{i}_k^{c,fault} \end{bmatrix} = \begin{bmatrix} \vec{i}_{k,re}^{a,fault} + j\vec{i}_{k,im}^{a,fault} \\ \vec{i}_{k,re}^{b,fault} + j\vec{i}_{k,im}^{b,fault} \\ \vec{i}_{k,re}^{c,fault} + j\vec{i}_{k,im}^{c,fault} \end{bmatrix} = - \begin{bmatrix} \left(\frac{p_{sub}^{a,mea} + jq_{sub}^{a,mea}}{\vec{v}_{sub}^{a,\eta}} \right)^* \\ \left(\frac{p_{sub}^{b,mea} + jq_{sub}^{b,mea}}{\vec{v}_{sub}^{b,\eta}} \right)^* \\ \left(\frac{p_{sub}^{c,mea} + jq_{sub}^{c,mea}}{\vec{v}_{sub}^{c,\eta}} \right)^* \end{bmatrix} + \frac{1}{2} \mathbf{Y}_{sub}^{sh} \begin{bmatrix} \vec{v}_{sub}^{a,\eta} \\ \vec{v}_{sub}^{b,\eta} \\ \vec{v}_{sub}^{c,\eta} \end{bmatrix} \quad (8)$$

where $\vec{i}_k^{j,fault}$ is the fault current injection of each phase j at bus k ; $p_{sub}^{j,mea}$ and $q_{sub}^{j,mea}$ are the active and reactive power injections of each phase j at the substation, respectively; and $\vec{v}_{sub}^{j,\eta}$ is the voltage phasor of each phase j at the substation and iteration η .

Since the angular reference is placed at an internal bus of the Thevenin equivalent described in Section II-D, the voltages at the substation and the fault currents are updated at every iteration η . In cases where the distribution network has DGs, the fault current is modeled as the summation of the contributions of all available power sources. An equation similar to (8) is applied to every DG.

Finally, given that these fault currents are indeed approximations of the actual fault currents, they are associated with small weights. This allows the residual associated with the fault currents to better fit the available measurements, improving the fault location accuracy. A discussion of the adequate weights is presented in Section IV.

III. PROPOSED FLA

The proposed approach is based on a search procedure composed of two stages: ① the identification of the faulted zone; and ② the identification of the faulted bus. The first stage consists of splitting the network into zones determined by boundary buses, which are the fork buses and terminal buses. This is done to reduce the computational burden of the searching procedure once just the boundary buses are tested at the first stage. An overview of the algorithm proposed to identify the faulted zones at the first stage is shown in Fig. 5.

According to Fig. 5, in the first step of the algorithm at the first stage, all the available conventional measurements provided by smart meters and the pseudo-measurements are fed to the BCBSE. The measurements are obtained during the fault, while the pseudo-measurements are obtained under pre-fault conditions. Recall that this is the best information available regarding unobservable areas of the distribution networks. In the second step, the network is split into zones de-

termined by boundary buses. Then, the first faulted boundary bus (bus i) is selected, and the fault current at this bus is specified according to (8). Given this, the proposed BCBSE is run, and the index $J_i(\mathbf{x})$ is calculated. This index quantifies how the measurements, the pseudo-measurements, and the supposed fault location fit the estimated state. Thus, the closer the bus i is to the fault location, the lower the index $J_i(\mathbf{x})$ is. This procedure is repeated only for the boundary buses to identify the most likely faulted zones.

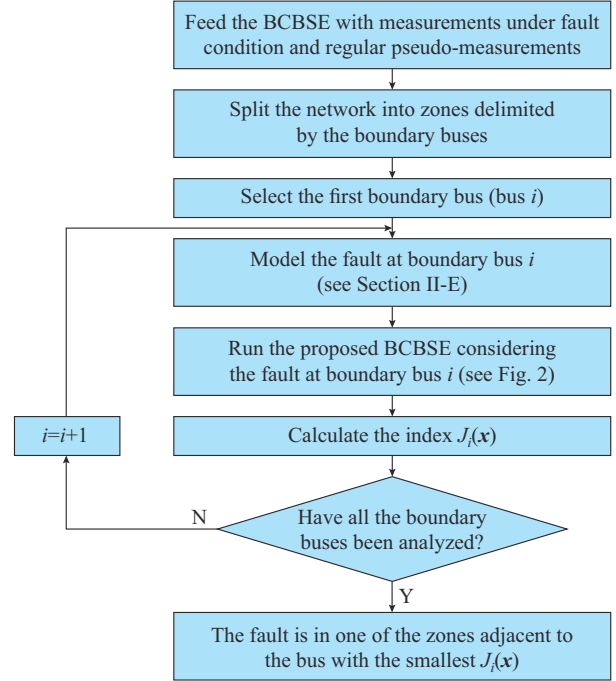


Fig. 5. Algorithm for identification of faulted zone at first stage.

After identifying the faulted zones, the BCBSE-based FLA is run for the buses of the most likely faulted zones, as proposed in Fig. 6.

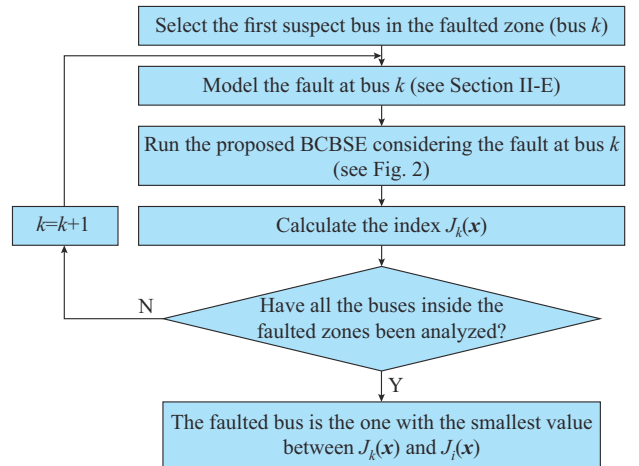


Fig. 6. Algorithm for fault location in faulted zone at second stage.

At the second stage, bus k (a bus inside the faulted zone) is selected as suspect bus and the fault currents are specified at this bus according to (8). Similar to the algorithm of Fig. 5, the proposed BCBSE is run, and the index $J_k(\mathbf{x})$ is calcu-

lated. The faulted bus is the one with the smallest $J_k(\mathbf{x})$.

Given that faults are more prone to occur on branches instead of buses, to improve the accuracy of the fault location, fictitious buses equally spaced can be placed on branches adjacent to the bus with the smallest $J_k(\mathbf{x})$, and the proposed approach can be run for these fictitious buses. However, it is worth mentioning that the spacing does not necessarily have to be fixed and can be of any size, that is, a finer or larger spacing. This will depend on the length of the branch. Given this, it is important to highlight that the smaller the distance between these fictitious buses, the greater the accuracy of the fault location. On the other hand, increasing the number of fictitious buses increases the computational burden. In practice, a distance from 50 to 100 m is recommended between fictitious buses. This is a typical distance among consecutive poles.

In cases where there are unobservable areas in the distribution networks, classical algorithms for observability analysis, as proposed in [23] or [24], can be used to define the exact set of required pseudo-measurements. However, in practice, pseudo-measurements associated with very low weights can be used at all buses [23], [24]. This avoids the usage of the observability analysis algorithms and does not significantly affect the accuracy of the proposed approach.

In this paper, the index $J(\mathbf{x})$, known as the weighted sum of squared residuals [23], is adopted as the fault location metric. To calculate $J(\mathbf{x})$, it is enough that the distribution network is minimally observable, i. e., the number of state variables is equal to that of available measurements (actual measurements, pseudo-measurements, virtual measurements, and constraints related to the reference bus) [23]. According to state estimation theory, this is the minimal amount of measurements required for state estimation purposes. The index $J_k(\mathbf{x})$ is calculated according to (9) using the estimates \mathbf{x}^{est} provided by the BCBSE with the fault placed at bus k , and the minimum value for $J_k(\mathbf{x})$ is the FLI, as shown in (10). Recall that this index is also used to identify the faulted zones.

$$J_k(\mathbf{x}) = (\mathbf{z}^{eq}(\mathbf{x}) - \mathbf{H}\mathbf{x}^{est})^T \mathbf{W} (\mathbf{z}^{eq}(\mathbf{x}) - \mathbf{H}\mathbf{x}^{est}) \quad (9)$$

$$FLI = \min\{J_k(\mathbf{x})\} \quad (10)$$

IV. CASE STUDIES

The proposed approach was implemented in MATLAB 2017b and the tests were run considering a modified version of the IEEE 34-bus distribution feeder [39]. In this modified version, voltage regulators were removed and the concept of dummy lines and dummy buses was adopted to represent single- and two-phase branches and buses as three-phase elements [36]. Moreover, some new buses were added in order to accommodate the distributed loads, in addition to Bus 0 included to represent the angular reference. The modified circuit resulted in a total of 52 buses, as shown in Fig. 7.

To simulate the measured values z_i^{true} , the fault, as well as the healthy network, was simulated on the software OpenDSS [40]. Fault scenarios were simulated varying: fault location, fault type, fault resistance, and the presence of distributed generators. All tests were performed on a personal

computer with i7-7500U 2.90 GHz CPU and 16 GB of RAM.

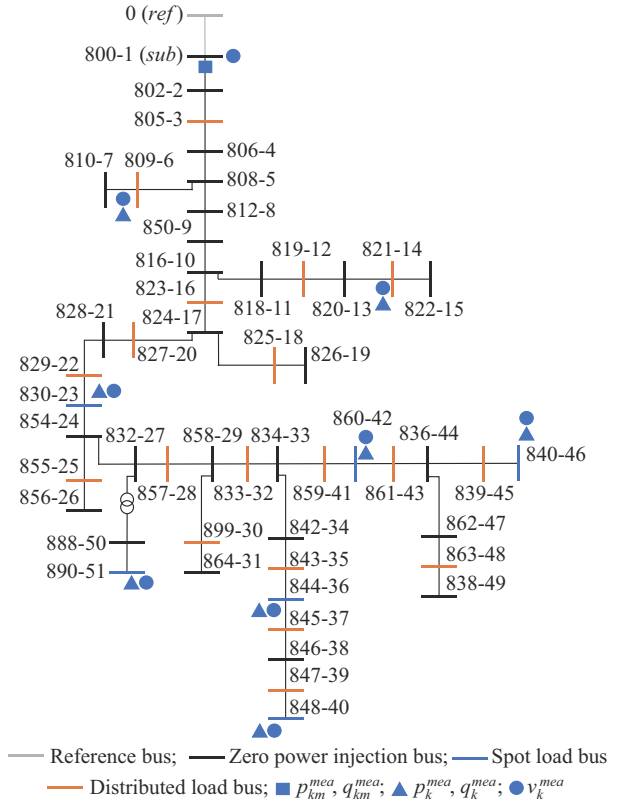


Fig. 7. Modified IEEE 34-bus distribution feeder.

To simulate the availability of actual measurement values z_i , deviations following normal distribution were added to the measured values z_i^{true} according to (11), where L_i is a normally distributed random variable with zero mean and unitary variance, i. e., $L_i \sim N(0, 1)$ [34]. The standard deviation σ_i for the i^{th} measurement is calculated according to (12), where z_i^{true} corresponds to the values obtained from OpenDSS, and E_{rror} is the maximum percentage error associated with the inaccuracy of measurement devices, instrument transformers, and communication infrastructure [41].

$$z_i = z_i^{true} + L_i \sigma_i \quad (11)$$

$$\sigma_i = \frac{z_i^{true} E_{rror}}{3 \times 100} \quad (12)$$

The initial measurement plan (Plan A) is depicted in Fig. 7. In this plan, six spot load buses (blue buses) and two distributed load buses (orange buses) have power and voltage magnitude measurements. Also, power flow and voltage measurements are considered at the substation bus, resulting in a total of 9 measured buses. The remaining buses (black buses) are zero power injection buses with the weight set to be 10^8 .

All these measurements are provided by smart meters, for which the E_{rror} on power and voltage measurements is 2% and 1%, respectively. The E_{rror} considered for pseudo-measurements is 50% over the true power injections obtained from the OpenDSS. The current injection representing the fault is associated with a small weight [42], [43], i. e., 10.

These weights are assessed and discussed later in this paper.

A second measurement plan (Plan B) containing twice the number of meters is also considered. The new measurements of power and voltage magnitude are placed at Buses 3, 16, 18, 20, 25, 28, 30, 32, and 48. The convergence criterion of the BCBSE is reached if the maximum absolute value of mismatches on the state variables is less than a specified tolerance, i.e., $\max|\mathbf{x}^{\eta+1} - \mathbf{x}^\eta| < \tau$, where the tolerance is $\tau = 10^{-5}$.

A. Impact of Angular Reference on BCBSE Under Fault Condition

In this subsection, the impact of the angular reference on the convergence of the BCBSE under fault conditions is assessed. Single- and three-phase faults are simulated since they represent the most frequent and severe faults, respectively. Three specifications of angular reference are considered.

1) Substation bus: the voltage magnitudes are measured by a smart meter and the angles are assumed to be 120° displaced at the substation.

2) Internal bus: the complex voltages present the same magnitude and the angles are 120° displaced at internal bus (bus behind the substation), as presented in Section II-D.

3) Substation bus (μ PMU): the voltage magnitudes and angles are provided by μ PMU at the substation bus.

For this purpose, the complex voltages estimated by the BCBSE ($\vec{\mathbf{v}}_n^{est}$) considering the three specifications of angular reference are assessed through the mean absolute error (MAE) according to (13), where $\vec{\mathbf{v}}_n^{true}$ is the measured complex voltage, and N_B is the number of buses in the network. The smaller the MAE, the better the estimates fit the available measurements.

$$MAE = \frac{1}{N_B} \sum_{n=1}^{N_B} \left| \frac{\vec{\mathbf{v}}_n^{true} - \vec{\mathbf{v}}_n^{est}}{\vec{\mathbf{v}}_n^{true}} \right| \quad (13)$$

Figures 8 and 9 show the MAE obtained considering single- and three-phase faults at Bus 22, respectively, and considering the two measurement plans with fault resistance varying from 1 to 100 Ω . As can be observed, greater MAEs are obtained when the angular reference is placed at the substation containing just a smart meter. Placing the angular reference at an internal bus and installing a μ PMU at the substation provides very similar MAEs. For instance, given a single-phase fault with the fault resistance of 1 Ω , the MAEs considering the specification of the angular reference at the internal bus and at the substation bus with μ PMU are 2.58×10^{-3} and 2.45×10^{-3} , respectively. On the other hand, considering the three-phase faults, the MAEs considering the three specifications of the angular reference present very similar values. This confirms the importance of the approach recommended in this paper to represent the angular reference, specially in the presence of asymmetrical faults. In both fault types, it is possible to observe that the MAE decreases as the number of measurements increases.

Considering the same simulation depicted in the previous paragraph, Figs. 10 and 11 show the number of iterations η required for the BCBSE to reach the convergence. During the simulation of the single-phase fault, when the angular reference is placed at the substation containing just a smart

meter, the number of iterations is the highest compared to the other two specifications. For instance, given a single-phase fault with the fault resistance of 1 Ω , the average numbers of iterations considering the angular reference at the internal bus and at the substation bus (μ PMU) are 7.45 and 5.50, respectively. On the other hand, when the angular reference at the substation bus containing just a smart meter is adopted, the average number of iterations reaches 11.45. As the fault resistance and the number of available measurements increase, the number of iterations decreases in both fault types.

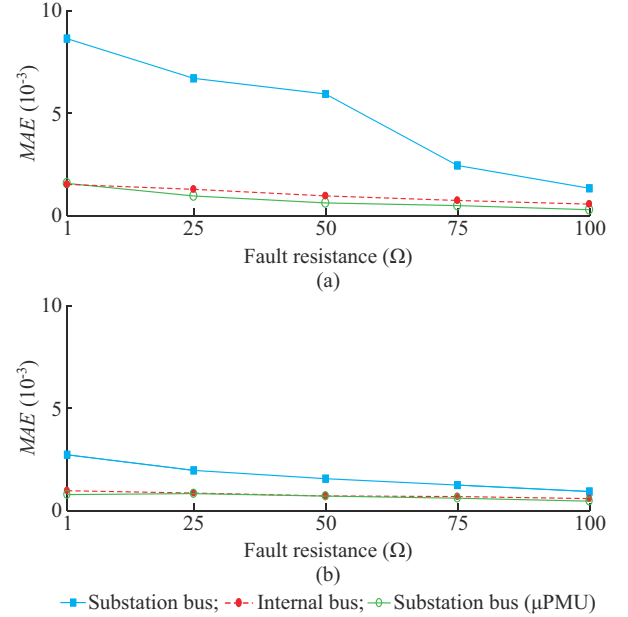


Fig. 8. MAE considering single-phase faults at Bus 22 with two measurement plans and fault resistance varying from 1 to 100 Ω . (a) Plan A. (b) Plan B.

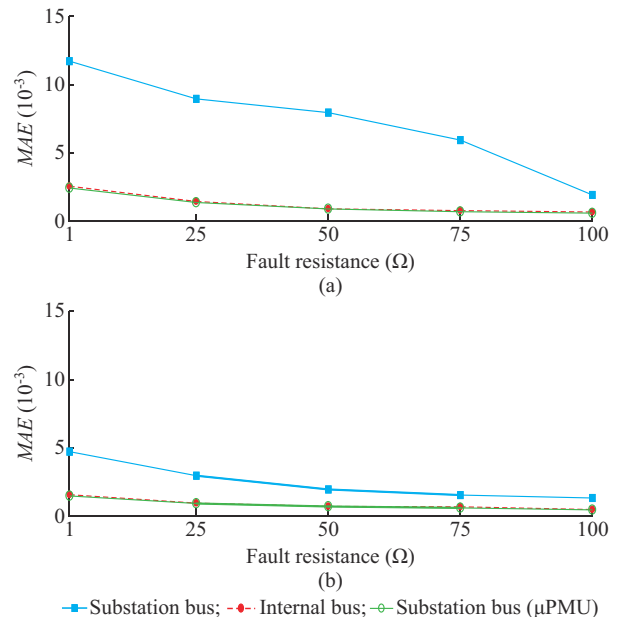


Fig. 9. MAE considering three-phase faults at Bus 22 with two measurement plans and fault resistance varying from 1 to 100 Ω . (a) Plan A. (b) Plan B.

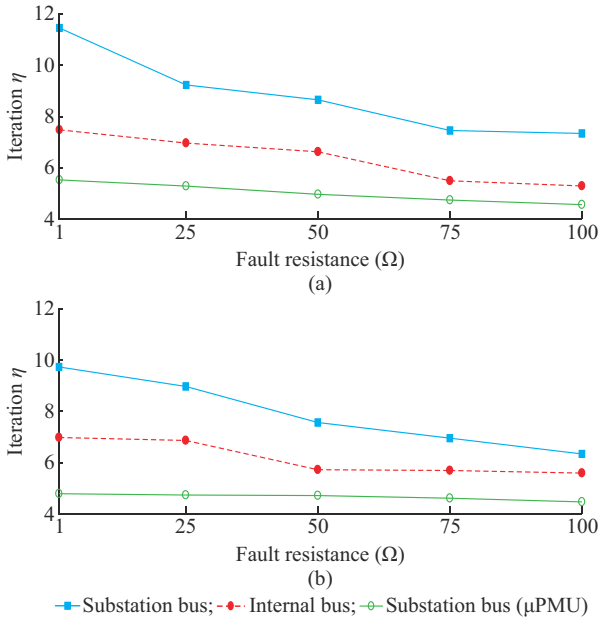


Fig. 10. Number of iterations considering single-phase faults at Bus 22 with two measurement plans and fault resistance varying from 1 to 100 Ω . (a) Plan A. (b) Plan B.

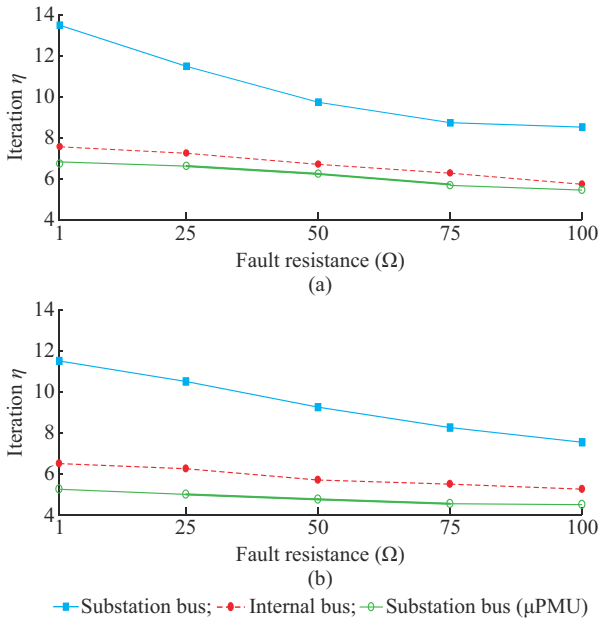


Fig. 11. Number of iterations considering three-phase faults at Bus 22 with two measurement plans and fault resistance varying from 1 to 100 Ω . (a) Plan A. (b) Plan B.

In summary, the proposed approach to represent the angular reference in the BCBSE under fault conditions can provide similar results to the adoption of a μ PMU at the substation with a significantly smaller cost. This approach shows the relevance with the accuracy of the BCBSE, specially in the presence of asymmetrical faults.

B. Assessment of BCBSE-based FLA

In this subsection, the performance of the proposed approach is assessed in terms of success percentage in correctly identifying the fault location, i.e., accuracy. Each fault sce-

nario is run 1000 times considering randomly defined noisy measurements. Single- and three-phase faults were simulated across the IEEE 34-bus distribution feeder considering fault resistance varying from 1 to 100 Ω . Tests were carried out considering fault resistance up to 1000 Ω , and the general conclusions are similar. These results are not presented for a matter of space.

As can be observed in Fig. 12(a), when the fault resistance is less than 70 Ω , the accuracy of the proposed approach is 100% for all single-phase faults. As the fault resistance increases, the accuracy of the proposed approach decreases up to 94% when the fault resistance reaches 100 Ω at Bus 49. The worst performances are observed at Buses 5, 21, 31, 33, and 49. It can be concluded that as the fault resistance increases, the accuracy slightly decreases. On the other hand, as can be observed by comparing Fig. 12(a) and (b), the accuracy increases as the number of measurements increases. Considering Plan B, the accuracy is 100% for all assessed scenarios.

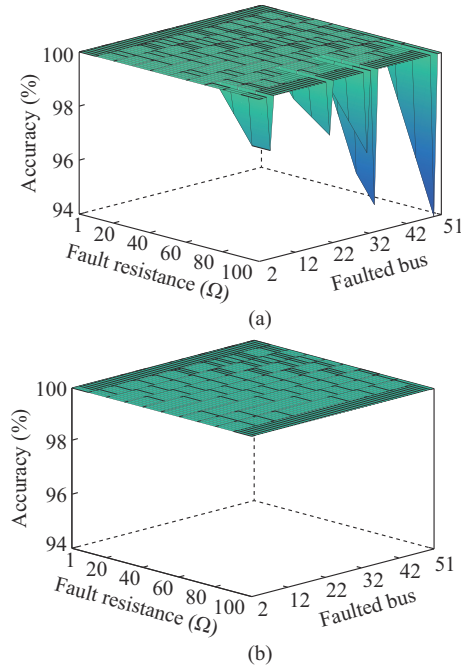


Fig. 12. Accuracy of proposed approach considering single-phase faults with Plan A and Plan B. (a) Plan A. (b) Plan B.

Similar behavior is presented by the proposed approach when three-phase faults are assessed. According to Fig. 13, when the fault resistance is 100 Ω , the accuracy of the proposed approach is 99% at Bus 5 and 98% at Buses 21 and 33. Again, the accuracy of the proposed approach increases as the number of measurements increases from Plan A to Plan B. Besides, tests were carried out considering two-phase faults, and the accuracies are similar.

C. Assessment of Proposed Approach Considering Fault on Branch

The previous analysis have considered faults at buses. However, it is well known that the faults are much more prone to occur on branches. To locate faults on branches, the proposed approach is run at the boundary buses in order to identify the faulted zones.

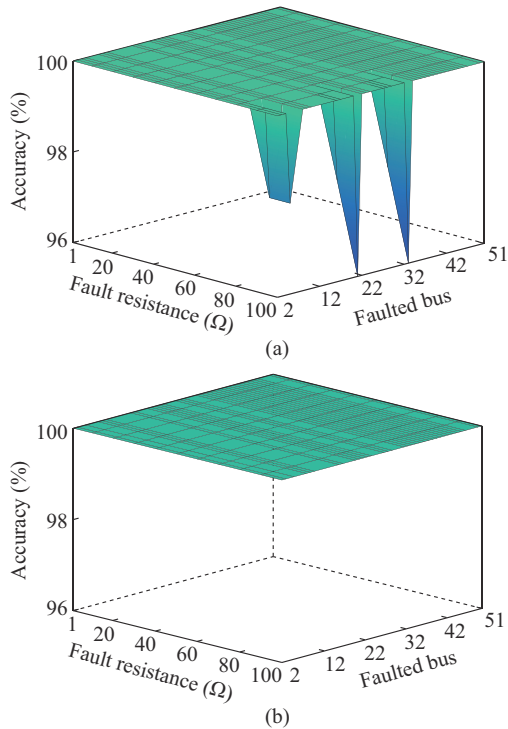


Fig. 13. Accuracy of proposed approach considering three-phase faults with Plan A and Plan B. (a) Plan A. (b) Plan B.

Then, it is run at buses belonging to these zones to identify the bus closest to the fault. Once the bus closest to the fault is located, the proposed approach is run on branches adjacent to this bus. These branches are examined by introducing a fictitious bus that sweeps them from the beginning to the end. Based on this procedure, single- and three-phase faults were assessed with fault resistance varying from 1 to 100 Ω on Branch 21-22, as shown in Fig. 14. The length of this branch is 3.1 km [39].

The measurement plan is Plan A. The performance assessment is performed in terms of the maximum error class considering 1000 sets of randomly defined noisy measurements that are produced for each fault scenario. For simplicity, the fictitious buses were spaced every 100 m far from each other. However, any distance between the fictitious buses can be adopted. When the fault resistance is less than 70 Ω , the accuracy of the proposed approach is between 0 and 100 m considering the single-phase fault, which means that the fault is between two consecutive fictitious buses. As the fault resistance increases, the accuracy of the proposed approach decreases. This can be observed, for instance, in the cases of single-phase faults with the resistance greater than 70 Ω . For the adopted spacing between the fictitious buses, the worst error was smaller than 300 m. Recall that these results can be improved by installing more meters. A similar behavior occurs with the three-phase faults, as shown in Fig. 14(b). In this case, the maximum error was less than 100 m for all assessed fault scenarios.

D. Assessment of Proposed Approach Considering Fault on Underground Cable Branch

A case study in a distribution network containing underground cables is presented in the following.

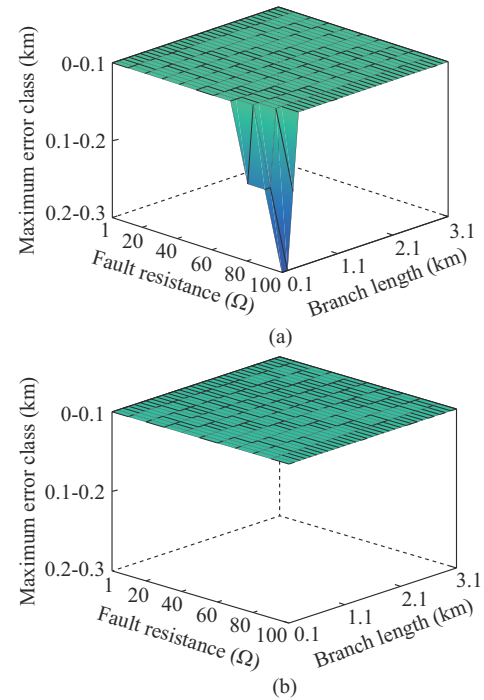


Fig. 14. Accuracy of proposed approach considering single- and three-phase faults on Branch 21-22. (a) Single-phase fault. (b) Three-phase fault.

This case study is based on the 37-bus test feeder. This feeder is an actual feeder in California, USA, with a 4.8 kV operating voltage. It is featured by delta configuration, all branch segments are underground, the substation voltage regulation is based on two single-phase open-delta regulators, spot loads, and very unbalanced [39]. The underground branch examined is Branch 702-703 with a length of 400 m approximately.

In this case, a fictitious bus containing the fault sweeps the branch from the beginning to the end. Based on this, single- and three-phase faults were assessed with the fault resistance varying from 1 to 100 Ω on Underground Branch 702-703, as shown in Fig. 15. In the measurement plan, 25 spot load buses have power and voltage magnitude measurements, and power flow and voltage measurements are considered at substation bus. The performance assessment is performed in terms of the maximum error class considering 1000 sets of randomly defined noisy measurements that are produced for each scenario. For simplicity, the fictitious buses were spaced every 20 m far from each other. However, any distance between the fictitious buses can be adopted.

When the fault resistance is less than 70 Ω , the accuracy of the proposed approach is between 0 and 20 m considering the single-phase fault. As the fault resistance increases, the accuracy of the proposed approach decreases. This can be observed, for instance, in the cases of single-phase faults with the resistance greater than 70 Ω . In the worst cases, the errors are smaller than 60 m. Keep in mind that these results can be improved by installing more meters. A similar behavior occurs with the three-phase faults, as can be observed in Fig. 15(b). In this case, the maximum error was smaller than 20 m for all assessed fault scenarios.

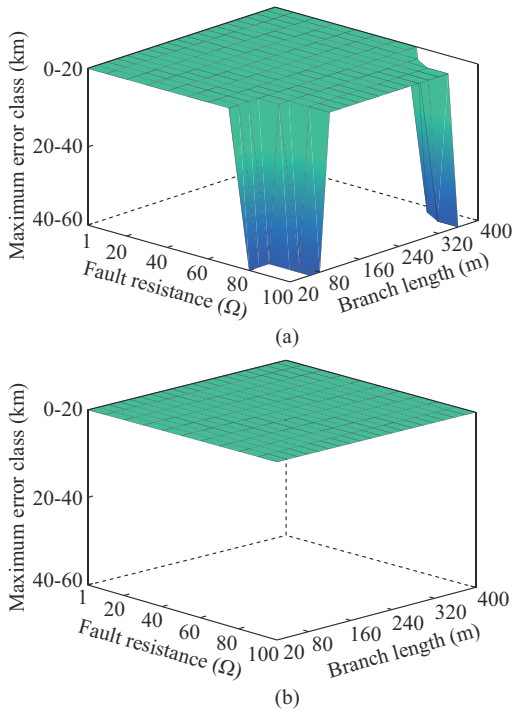


Fig. 15. Accuracy of proposed approach considering single- and three-phase faults on Underground Branch 702-703. (a) Single-phase fault. (b) Three-phase fault.

E. Assessment of Proposed Approach Considering DG

In this subsection, the proposed approach is assessed in the presence of DGs. For that, three distributed generators were added at Buses 14, 40, and 46 (two synchronous generators at Buses 14 and 40 and one PV at Bus 46 [21]) of the test system shown in Fig. 7. Plan A was considered. The capacity of each DG is 500 kVA. It is worth mentioning that the fault current now is the contribution not only of the current of the substation but also of the DG.

As can be observed in Fig. 16, when the fault resistance is less than 70Ω , the accuracy of the proposed approach is 100% for the single-phase fault. As the fault resistance increases, the accuracy of the proposed approach decreases. For instance, in the case of a single-phase fault with the fault resistance greater than 70Ω and 80Ω at Buses 5 and 31, respectively, the accuracy decreases up to 98% in both buses. Besides, it is possible to observe that, despite keeping the same number of measurements (Plan A), with the help to the contribution of more power sources to the fault, the accuracy of the proposed approach improves. In cases of three-phase faults in the presence of DGs, the accuracy is 100% regardless of the fault location and resistance.

F. Assessment of Weights on Proposed Approach

In the previous subsections, the weights of the measurements and pseudo-measurements were set according to (11) and (12). The weights of the zero injections and the fault current were set to be 10^8 and 10, respectively. These values were chosen from the experience of the authors with state estimation and FLAs. In this subsection, a sensitivity study on these weights is presented.

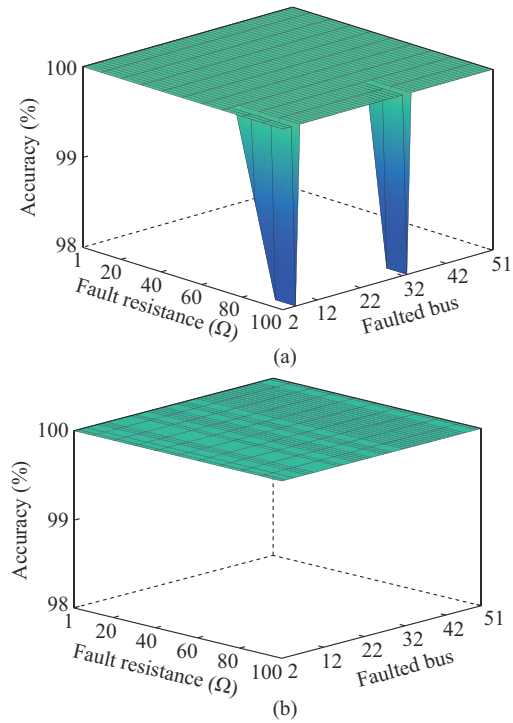


Fig. 16. Accuracy of proposed approach considering single- and three-phase faults with presence of DG. (a) Single-phase fault. (b) Three-phase fault.

In the first case, a single-phase fault was applied across the test system considering different weights to the pseudo-measurements and the fault current. The Plan A was considered. For each fault scenario, a total of 1000 sets of noisy measurements were produced and assessed. Figure 17 shows the accuracy of the proposed approach.

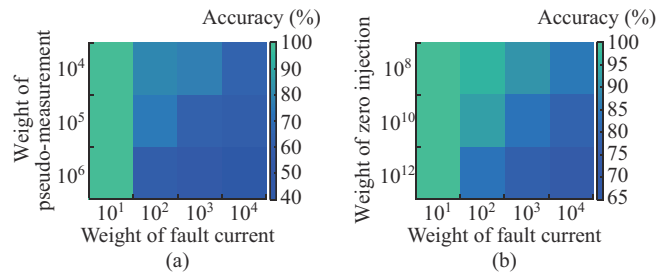


Fig. 17. Accuracy of proposed approach considering weight influence of pseudo-measurement and zero injection versus fault current. (a) Weight influence of pseudo-measurement versus fault current. (b) Weight influence of zero injection versus fault current.

In Fig. 17(a), the weight of the zero injections is set in 10^8 . The weight of the pseudo-measurements ranges from 10^4 to 10^6 , and the weight of the fault current ranges from 10 to 10^4 . As it is possible to be observed, when the weight of the fault current is set to be 10, the accuracy of the proposed approach does not decrease regardless of the weight of the pseudo-measurements. As the weight of the fault current increases, the accuracy of the proposed approach deteriorates up to 40%. It is worth mentioning that a fair weight for the pseudo-measurements would be around 10^4 .

In Fig. 17(b), the weight of the zero injections ranges

from 10^8 to 10^{12} , while the weight of the fault currents ranges from 10 to 10^4 . The weight of the pseudo-measurements is set to be 10^4 . As it can be observed, when the weight of the fault currents is 10, the accuracy of the proposed approach does not decrease regardless of the weight of the zero injections. Besides, as the weight of the zero injections and the weight of the fault currents increase, it is possible to observe that the accuracy of the proposed approach deteriorates up to 65%.

Based on the results shown in this subsection, the range for the specification of the weights is wide. This simplifies the choice of suitable weights for the proposed approach. Besides, this indicates that from a reduced set of simulations, these weights can be properly set.

V. CONCLUSION

Due to the errors inherent to the measurements, the delays in communication, the limited number of available measurements (leading to the adoption of pseudo-measurements), the presence of distributed generators, the required three-phase representation of the distribution feeders, and the typical unbalanced loads, the state estimation approaches are promising as the main core for FLAs. In this paper, the proposed FLA is based on an improved BCBSE, in which the Jacobian matrix remains constant throughout the solution process, reducing the computational burden of the FLA. However, the computational time is not a hard constraint for FLAs. Moreover, the proposed approach allows the accurate locating of faults at buses or branches without requiring measurements from PMUs. The use of the PMUs is the most common requirement of the more recent approaches for fault location based on SEs.

In summary, the proposed FLA can use measurements from PMUs, however, this is not a requirement. Indeed, the proposed approach can be applied given a reduced set of conventional non-synchronized measurements. However, similar to approaches based on measurements, increasing the number of available measurements increases the robustness and accuracy of the proposed approach.

As shown in the results, the improved BCBSE can be successfully applied to faulted three-phase distribution networks mainly due to: ① the way the angular reference is modeled; ② the way the faulted bus is represented; ③ the proper weights assigned for the measurements and pseudo-measurements; and ④ the representation of all shunt admittances at buses and branches in modeling of equivalent current measurements. These modeling aspects can be adopted regardless of the networks. Therefore, these are not conditions required to the proposed approach to gain a good performance, but they are modeling aspects that are usually disregarded when the SE is being applied in healthy networks. These modeling aspects are recommended in this paper to be adopted in faulted networks achieving high accuracy in fault location without requiring measurements from PMUs.

In order to assess the performance of the proposed approach, several properly designed fault scenarios, using Monte Carlo simulations, were run on the IEEE 34-bus distribution feeder and the 37-bus distribution feeder (with overhead

and underground branches, respectively). Results indicate that the proposed approach is an accurate and efficient alternative to the available approaches without the need of adopting phasor measurements.

Similar to all FLAs based on measurements and network analysis tools (short-circuit, load flow, and state estimation), in the proposed approach, the accuracy of the fault location depends on the number and location of the available measurements. In addition, these FLAs based on network analysis tools usually can present difficulties to converge in networks that have very high grounding impedances as well as in ungrounded systems.

REFERENCES

- [1] F. Shen, Q. Wu, and Y. Xue, "Review of service restoration for distribution networks," *Journal of Modern Power Systems and Clean Energy*, vol. 8, no. 1, pp. 1-14, Jan. 2019.
- [2] C. D'Adamo, S. Jupe, and C. Abbey, "Global survey on planning and operation of active distribution networks – update of CIGRE C6.11 working group activities," in *Proceedings of CIRED 2009 – 20th International Conference and Exhibition on Electricity Distribution – Part 1*, Prague, Czech Republic, Jun. 2009, pp. 1-4.
- [3] R. H. Salim, M. Resener, A. D. Filomena *et al.*, "Extended fault-location formulation for power distribution systems," *IEEE Transactions on Power Delivery*, vol. 24, no. 2, pp. 508-516, Apr. 2009.
- [4] S. Das, N. Karnik, and S. Santoso, "Distribution fault-locating algorithms using current only," *IEEE Transactions on Power Delivery*, vol. 27, no. 3, pp. 1144-1153, Apr. 2012.
- [5] H. Mirshekali, R. Dashti, A. Keshavarz *et al.*, "A novel fault location methodology for smart distribution networks," *IEEE Transactions on Smart Grid*, vol. 12, no. 2, pp. 1277-1288, Mar. 2021.
- [6] F. Aboshady, D. Thomas, and M. Sumner, "A new single end wide-band impedance based fault location scheme for distribution systems," *Electric Power Systems Research*, vol. 173, pp. 263-270, Aug. 2019.
- [7] K. Jia, T. Bi, Z. Ren *et al.*, "High frequency impedance based fault location in distribution system with DGs," *IEEE Transactions on Smart Grid*, vol. 9, no. 2, pp. 807-816, Mar. 2018.
- [8] A. Borghetti, M. Bosetti, C. Nucci *et al.*, "Integrated use of time-frequency wavelet decompositions for fault location in distribution networks: theory and experimental validation," *IEEE Transactions on Power Delivery*, vol. 25, no. 4, pp. 3139-3146, Apr. 2010.
- [9] S. Robson, A. Haddad, and H. Griffiths, "Fault location on branched networks using a multiended approach," *IEEE Transactions on Power Delivery*, vol. 29, no. 4, pp. 1955-1963, Jun. 2014.
- [10] L. Xie, L. Luo, Y. Li *et al.*, "A traveling wave-based fault location method employing VMD-TEO for distribution network," *IEEE Transactions on Power Delivery*, vol. 35, no. 4, pp. 1987-1998, Aug. 2020.
- [11] E. C. Maritz, J. M. Maritz, and M. Salehi, "A travelling wave-based fault location strategy using the concepts of metric dimension and vertex covers in a graph," *IEEE Access*, vol. 9, pp. 155815-155825, Nov. 2021.
- [12] A. Tashakkori, P. J. Wolfs, S. Islam *et al.*, "Fault location on radial distribution networks via distributed synchronized traveling wave detectors," *IEEE Transactions on Power Delivery*, vol. 35, no. 3, pp. 1553-1562, Jun. 2020.
- [13] D. Thukaram, H. Khincha, and H. Vijaynarasimha, "Artificial neural network and support vector machine approach for locating faults in radial distribution systems," *IEEE Transactions on Power Delivery*, vol. 20, no. 2, pp. 710-721, Apr. 2005.
- [14] M. Pourahmadi-Nakhli and A. A. Safavi, "Path characteristic frequency-based fault locating in radial distribution systems using wavelets and neural networks," *IEEE Transactions on Power Delivery*, vol. 26, no. 2, pp. 772-781, Apr. 2011.
- [15] W.-H. Kim, J.-Y. Kim, W.-K. Chae *et al.*, "LSTM-based fault direction estimation and protection coordination for networked distribution system," *IEEE Access*, vol. 10, pp. 40348-40357, Apr. 2022.
- [16] Y. Jiang, "Data-driven fault location of electric power distribution systems with distributed generation," *IEEE Transactions on Smart Grid*, vol. 11, no. 1, pp. 129-137, Jan. 2020.
- [17] Y. Jiang, "Data-driven probabilistic fault location of electric power distribution systems incorporating data uncertainties," *IEEE Transactions on Smart Grid*, vol. 12, no. 5, pp. 4522-4534, Apr. 2021.

- [18] R. A. F. Pereira, L. G. W. da Silva, M. Kezunovic *et al.*, "Improved fault location on distribution feeders based on matching during-fault voltage sags," *IEEE Transactions on Power Delivery*, vol. 24, no. 2, pp. 852-862, Mar. 2009.
- [19] F. C. Trindade, W. Freitas, and J. C. Vieira, "Fault location in distribution systems based on smart feeder meters," *IEEE Transactions on Power Delivery*, vol. 29, no. 1, pp. 251-260, Feb. 2014.
- [20] K. Jia, B. Yang, T. Bi *et al.*, "An improved sparse-measurement-based fault location technology for distribution networks," *IEEE Transactions on Industrial Informatics*, vol. 17, no. 3, pp. 1712-1720, May 2020.
- [21] M. Majidi and M. Etezadi-Amoli, "A new fault location technique in smart distribution networks using synchronized/nonsynchronized measurements," *IEEE Transactions on Power Delivery*, vol. 33, no. 3, pp. 1358-1368, Dec. 2017.
- [22] K. Jia, B. Yang, X. Dong *et al.*, "Sparse voltage measurement-based fault location using intelligent electronic devices," *IEEE Transactions on Smart Grid*, vol. 11, no. 1, pp. 48-60, Jan. 2020.
- [23] A. Monticelli, *State Estimation in Electric Power Systems: a Generalized Approach*. Berlin: Springer Science & Business Media, 2012.
- [24] A. Abur and A. G. Exposito, *Power System State Estimation: Theory and Implementation*. Bath: CRC press, 2004.
- [25] M. Pignati, L. Zanni, P. Romano *et al.*, "Fault detection and faulted line identification in active distribution networks using synchrophasor-based real-time state estimation," *IEEE Transactions on Power Delivery*, vol. 32, no. 1, pp. 381-392, Feb. 2017.
- [26] M. U. Usman and M. O. Faruque, "Validation of a PMU-based fault location identification method for smart distribution network with photovoltaics using real-time data," *IET Generation, Transmission & Distribution*, vol. 12, no. 21, pp. 5824-5833, Oct. 2018.
- [27] M. Gholami, A. Abbaspour, M. Moeini-Aghtaie *et al.*, "Detecting the location of short-circuit faults in active distribution network using PMU-based state estimation," *IEEE Transactions on Smart Grid*, vol. 11, no. 2, pp. 1396-1406, Mar. 2020.
- [28] Y. Zhang, J. Wang, and M. E. Khodayar, "Graph-based faulted line identification using micro-PMU data in distribution systems," *IEEE Transactions on Smart Grid*, vol. 11, no. 5, pp. 3982-3992, Sept. 2020.
- [29] F. Conte, F. D'Agostino, B. Gabriele *et al.*, "Fault detection and localization in active distribution networks using optimally placed phasor measurements units," *IEEE Transactions on Power Systems*, vol. 38, no. 1, pp. 714-727, Jan. 2023.
- [30] S. Jamali and A. Bahmanyar, "A new fault location method for distribution networks using sparse measurements," *International Journal of Electrical Power & Energy Systems*, vol. 81, pp. 459-468, Oct. 2016.
- [31] J. Cordova and M. O. Faruque, "Fault location identification in smart distribution networks with distributed generation," in *Proceedings of 2015 North American Power Symposium (NAPS)*, Charlotte, USA, Oct. 2015, pp. 1-7.
- [32] S. Jamali, A. Bahmanyar, and E. Bompard, "Fault location method for distribution networks using smart meters," *Measurement*, vol. 102, pp. 150-157, May 2017.
- [33] M. E. Baran and A. W. Kelley, "A branch-current-based state estimation method for distribution systems," *IEEE Transactions on Power Systems*, vol. 10, no. 1, pp. 483-491, Feb. 1995.
- [34] M. C. de Almeida and L. F. Ochoa, "An improved three-phase AMB distribution system state estimator," *IEEE Transactions on Power Systems*, vol. 32, no. 2, pp. 1463-1473, Mar. 2017.
- [35] L. F. Ugarte, J. Tuo, and M. C. de Almeida, "Assessing approaches to modeling voltage magnitude measurements in state estimators devoted to active distribution networks," *Electric Power Systems Research*, vol. 200, p. 107440, Nov. 2021.
- [36] M. Abdel-Akher and K. M. Nor, "Fault analysis of multiphase distribution systems using symmetrical components," *IEEE Transactions on Power Delivery*, vol. 25, no. 4, pp. 2931-2939, Oct. 2010.
- [37] D. A. Haughton and G. T. Heydt, "A linear state estimation formulation for smart distribution systems," *IEEE Transactions on Power Systems*, vol. 28, no. 2, pp. 1187-1195, May 2013.
- [38] R. S. da Silva, T. R. Fernandes, and M. C. de Almeida, "Specifying angular reference for three-phase distribution system state estimators," *IET Generation, Transmission & Distribution*, vol. 12, no. 7, pp. 1655-1663, Feb. 2018.
- [39] W. H. Kersting, "Radial distribution test feeders," *IEEE Transactions on Power Systems*, vol. 6, no. 3, pp. 975-985, Aug. 1991.
- [40] R. C. Dugan and T. E. McDermott, "An open source platform for collaborating on smart grid research," in *Proceedings of 2011 IEEE PES General Meeting*, , Detroit, USA, Jul. 2011, pp. 1-7.
- [41] P. A. Cavalcante and M. C. de Almeida, "Fault location approach for distribution systems based on modern monitoring infrastructure," *IET Generation, Transmission & Distribution*, vol. 12, no. 1, pp. 94-103, Oct. 2017.
- [42] A. Abur, "A bad data identification method for linear programming state estimation," *IEEE Transactions on Power Systems*, vol. 5, no. 3, pp. 894-901, Aug. 1990.
- [43] US Department of Energy, "Contribution to power system state estimation and transient stability analysis," Tech. Rep. DOE/ET/29362-1, Feb. 1984.

Luis F. Ugarte received the M.Sc. degree in electrical engineering from the State University of Campinas, Campinas, Brazil, in 2018, where he is currently working toward the Ph.D. degree. His research interests include electrical mobility, power system analysis, and sustainability energy.

Madson C. de Almeida received the Ph.D. degree from the State University of Campinas, Campinas, Brazil, in 2007. Currently, he is an Associate Professor at the State University of Campinas. His research interests include electrical mobility, distribution systems, grid edge technologies, and sustainability.

Luís H. T. Bandória received the M.Sc. degree in electrical engineering from the State University of Campinas, Campinas, Brazil, in 2021, where he is currently working toward the Ph.D. degree. His research interests include computational methods for power system analysis, grid edge technologies, sustainability and deep learning techniques devoted to power systems.